Development 139, 1691-1699 (2012) doi:10.1242/dev.072702

Turning gene function ON and OFF using sense and antisense photo-morpholinos in zebrafish

Alexandra Tallafuss[1,*], Dan Gibson[1], Paul Morcos[2], Yongfu Li[2], Steve Seredick[1], Judith Eisen[1] and Philip Washbourne[1,*]

SUMMARY

To understand the molecular mechanisms of development it is essential to be able to turn genes on and off at will and in a spatially restricted fashion. Morpholino oligonucleotides (MOs) are very common tools used in several model organisms with which it is possible to block gene expression. Recently developed photo-activated MOs allow control over the onset of MO activity. However, deactivation of photo-cleavable MO activity has remained elusive. Here, we describe photo-cleavable MOs with which it is possible to activate or de-activate MO function by UV exposure in a temporal and spatial manner. We show, using several different genes as examples, that it is possible to turn gene expression on or off both in the entire zebrafish embryo and in single cells. We use these tools to demonstrate the sufficiency of *no tail* expression as late as tailbud stage to drive medial precursor cells towards the notochord cell fate. As a broader approach for the use of photo-cleavable MOs, we show temporal control over *gal4* function, which has many potential applications in multiple transgenic lines. We demonstrate temporal manipulation of Gal4 transgene expression in only primary motoneurons and not secondary motoneurons, heretofore impossible with conventional transgenic approaches. In another example, we follow and analyze neural crest cells that regained *sox10* function after deactivation of a photo-cleavable *sox10*-MO at different time points. Our results suggest that *sox10* function might not be critical during neural crest formation.

KEY WORDS: Morpholinos, MO, Zebrafish, *ntla*, UV, Photo-MO, Photo-cleavable, Gal4, GFP, *sox10*

INTRODUCTION

Unraveling the mechanisms underlying development requires availability of molecular tools with which to analyze the impact of gene function in detail. These tools should enable manipulation of gene function in specific tissues at a chosen time point during development. In zebrafish, one of the most commonly used tools to manipulate gene function is antisense morpholino oligonucleotides (MOs) that bind to mRNA. They can be targeted either to prevent translation initiation or to cause incorrect splicing by blocking splice site acceptors or donors, often resulting in non-functional proteins (Bill et al., 2009). Recently, different modified oligonucleotides were reported that temporarily block the binding capability of MOs (Deiters et al., 2010; Shestopalov and Chen, 2010). Furthermore, chemical substrates incorporated into the sequence of MOs were developed to regulate their activity (Tomasini et al., 2009). Exposure to UV light releases the MO, thus enabling temporal control over gene function. In addition, spatial control can be achieved by limiting light exposure to only small groups of cells (Shestopalov et al., 2007). Although these tools are available to turn off gene function at a chosen time point, turning on previously blocked endogenous gene function later in development, has not been feasible [however, see Clark et al. (Clark et al., 2011)].

We describe the capability and reliability of antisense photo-MOs (AS-photo-MOs), whose block of expression is released upon UV exposure, and complementary sense photo-MOs (S-photo-MOs), which maintain regular MOs in an inactive state until UV exposure, both throughout the embryo or restricted to single cells. We report three distinct strategies to examine feasibility of photo-cleavable MOs in assessing gene or cellular function: (1) we use spatiotemporal regulation of the *no tail* (*ntla*) gene to determine sufficiency of Ntla for notochord induction, (2) we regulate temporal expression of Gal4 to restrict expression of transgenes to a specific cell population, and (3) we use temporal regulation of the *sox10* gene to examine necessity for neural crest formation.

ntla encodes a T-box transcription factor (Schulte-Merker et al., 1994) expressed by a medial precursor cell (MPC) population and is required for formation of notochord and for posterior somite development (Amacher et al., 2002; Halpern et al., 1993). Zebrafish embryos lacking Ntla form floor plate (fp) at the expense of notochord, which results in a difference in muscle segment shape and a lack of muscle pioneer cell development (Halpern et al., 1993). *ntla* was shown to act cell autonomously to prevent notochord cell precursors from becoming fp, but non-cell-autonomously in development of posterior somites (Martin and Kimelman, 2008). Here, we used photo-MOs to confirm late gastrulation as a time point in development at which *ntla* is sufficient to induce notochord.

We considered photo-MOs as a useful tool for the restriction of transgene expression within the modular Gal4-UAS system (Halpern et al., 2008). Recently, new methods in the zebrafish were developed that allow temporal control over Gal4 expression, such

[1]Institute of Neuroscience, University of Oregon, 97403 Eugene, OR, USA. [2]Gene Tools, LLC, 1001 Summerton Way, 97370 Philomath, OR, USA.

*Authors for correspondence (tallafuss@uoneuro.uoregon.edu; pwash@uoneuro.uoregon.edu)

Accepted 22 February 2012

as ecdysone receptor fusions (Esengil et al., 2007) or MAZe (Collins et al., 2010); however, a large number of already established transgenic lines using Gal4-VP16 cannot be regulated by these new methods (see Faucherre and Lopez-Schier, 2011). As an example, we show temporal control over GFP expression, mediated by regulating the activator Gal4, in early developing primary motoneurons (PMNs), but not later developing secondary motoneurons (SMNs). This has not been possible until now as promoters or tools to drive gene expression in only PMNs are not available. Our results suggest that photo-cleavable MOs could be used not just to follow fluorescent protein expression but also to manipulate other transgene expression in PMNs using different UAS-dependent effector lines.

Furthermore, as an approach to distinguish between early and late gene function, we chose to study *sox10*, which is implicated in neural crest development and migration (Kelsh, 2006). However, it is unclear whether *sox10* is necessary for neural crest formation or maintenance (Carney et al., 2006). We use *sox10*-AS-photo-MOs to temporarily block *sox10* function and allow *sox10* to be expressed at different time points during development. Our results suggest that *sox10* might be unnecessary for early neural crest formation, but is indispensable for later neural crest development.

In summary, we take advantage of photo-cleavable *ntla*-AS-photo-MOs that are inactivated upon light exposure thereby allowing protein synthesis, and complementary *ntla*-S-photo-MOs that release *ntla*-MO when photo-cleaved. We describe cell fate choice of MPCs with temporally regulated depletion of *ntla* function, previously requiring technically more challenging cell transplant experiments. Furthermore, we show temporal control of the Gal4-UAS system, allowing manipulation of gene function in many already available transgenic lines. We provide evidence to support the hypothesis that *sox10* might not be required for neural crest formation but is important for later steps during neural crest development.

MATERIALS AND METHODS

Animal husbandry and lines

Zebrafish embryos were obtained from natural spawning of AB or AB/TU wild-type or Tg(hsp70:Gal4-VP16), Tg(UAS:GFP)kca33/+, Tg[(mnx1:Gal4-VP16)b1222,UAS:GFP], Et[(–1.5hsp70l:Gal4-VP16)s1102t,(UAS-E1b:Kaede)s1999t] and Tg(3.1neurog1:GFP)sb2 transgenic lines (see http://zfin.org/). Fish were staged by hours post-fertilization (hpf) at 28.5°C (Kimmel et al., 1995). All procedures were carried out in compliance with guidelines of the University of Oregon Animal Care and Use Committee.

MOs, photo-MOs and light exposure

All MOs and photo-MOs were obtained from Gene Tools, LLC. See supplementary material Fig. S1 for more information on photo-MO synthesis. We used *ntla*-MOs NT2 for all *ntla* experiments unless otherwise stated and *gal4*-MOs, *gfp*-MOs and *sox10*-MOs as described in the text (for sequences, see supplementary material Table S1). For all experiments, the lowest effective concentration was used as determined by titration experiments followed by morphological examination (see supplementary material Table S1), either with or without a fluorescein-tag that allowed monitoring distribution and uptake of the MO into the embryo. *ntla*-MO and *ntla*-S-photo-MO or *gal4*-MO and *gal4*-S-photo-MO were mixed to give working stock solutions, which were maintained in the dark at 25°C. No precautions concerning light exposure were made while manipulating embryos.

For light exposure, embryos were placed in a petri dish and illuminated with a broad spectrum mercury light source (HBO 100), comprising UV light with an intensity of 66 mW/cm^2 for 5-10 minutes using a Zeiss Lumar stereoscope (Thornwood, NY, USA) or with UV light (365 nm) with an intensity of 0.84 mW/cm^2 from a monochromator (TILL Photonics). Both conditions resulted in similar photo-MO function and the stereoscope was used for most experiments. For single-cell experiments, embryos were mounted at 11 hpf, dorsal side up. Laser-mediated cleavage of photo-MOs was performed using a 365 nm dye laser (VSL-337ND, Laser Science) on an upright microscope (Zeiss) with a 50× water immersion objective (Leitz).

Immunohistochemistry

Immunohistochemistry was carried out according to standard protocols (Westerfield, 2000). The following antibodies were used: anti-Ntla (1:1000) (Schulte-Merker et al., 1992), anti-Alcama (1:4000) (Trevarrow et al., 1990), anti-Gfap (zrf-1, 1:100) (Marcus and Easter, 1995), chicken anti-GFP (Millipore; 1:1000). Primary antibodies were revealed using secondary antibodies coupled to Alexa-Fluor dyes (goat anti-chicken, goat anti-rabbit, goat anti-mouse; 1:750, Life Technologies).

Embryos were scored and imaged on an inverted Nikon TU-2000 microscope with an EZ-C1 confocal system (Nikon) using a 40× objective or a 60× water immersion objective, or viewed with a Zeiss Axioplan2 microscope and photographed with a Zeiss AxioCam MRc5 camera.

RESULTS

We used cleavable MOs that incorporate a photo-sensitive subunit in the middle of the MO (Fig. 1A,B). The photo-subunit was synthesized to closely match spacing of an MO subunit in terms of bond distance so that MO activity is minimally compromised (Fig. 1C; supplementary material Fig. S1). Exposure to UV light results in cleavage of the photo-MO into two inactive fragments (Fig. 1A,B). AS-photo-MOs disrupt gene function by binding target RNA. However, their activity is rendered UV-sensitive by the photo-subunit (Fig. 1A) (Bill et al., 2009). By contrast, S-photo-MOs bind to and block MOs. These are then released upon light exposure, allowing the MO to become active and to block gene function (Fig. 1B) (see also Deiters et al., 2010; Shestopalov et al., 2007).

We tested the activity of translation-blocking *ntla*-S-photo-MOs and *ntla*-AS-photo-MOs in zebrafish embryos. We selectively used a wavelength of 365 nm (UV) or broad spectrum light sources, commonly used for fluorescence microscopy, to cleave the photo-subunit. It has been reported that high doses of UV light can cause severe damage in developing zebrafish embryos (Dong et al., 2007; Strahle and Jesuthasan, 1993), which manifested as ventralization and incomplete gastrulation. We tested embryos at different time points from the 16-cell stage (1.5 hpf) to late gastrulation (11 hpf) for UV sensitivity. We found that younger embryos are more sensitive to UV damage and we therefore delayed UV illumination until 5 hpf. MO-injected embryos tolerated >10 minutes of UV illumination without developing any signs of UV damage, similar to uninjected control embryos (Fig. 1D).

We analyzed binding and release abilities of *ntla*-photo-MOs in vivo by monitoring morphologically distinct phenotypes. We injected embryos at the single-cell stage, exposed them to UV at 5 hpf and assessed their phenotype at 1 dpf (Fig. 1F-I) or 2 dpf (Fig. 1D,E). We categorized phenotype severity into four different classes: severe, medium, mild and normal (Fig. 1F-I). Severe includes truncated, missing tail and notochord with u-shaped rather than chevron-shaped muscle segments. Embryos categorized as medium form a short tail and lack notochord, whereas mildly affected embryos have a normal but slightly shorter tail and develop notochord and fp similar to control embryos. We confirmed the morphologically observed phenotypes with target gene knockdown by Ntla antibody labeling (Fig. 1F-I) (Schulte-Merker et al., 1994).

Binding and dissociation properties of sense and antisense photo-MOs

MOs have been optimized for efficient binding to mRNA and generally have a length of 25 nucleotides. We tested S- and AS-photo-MOs of different lengths and with introduced mismatched

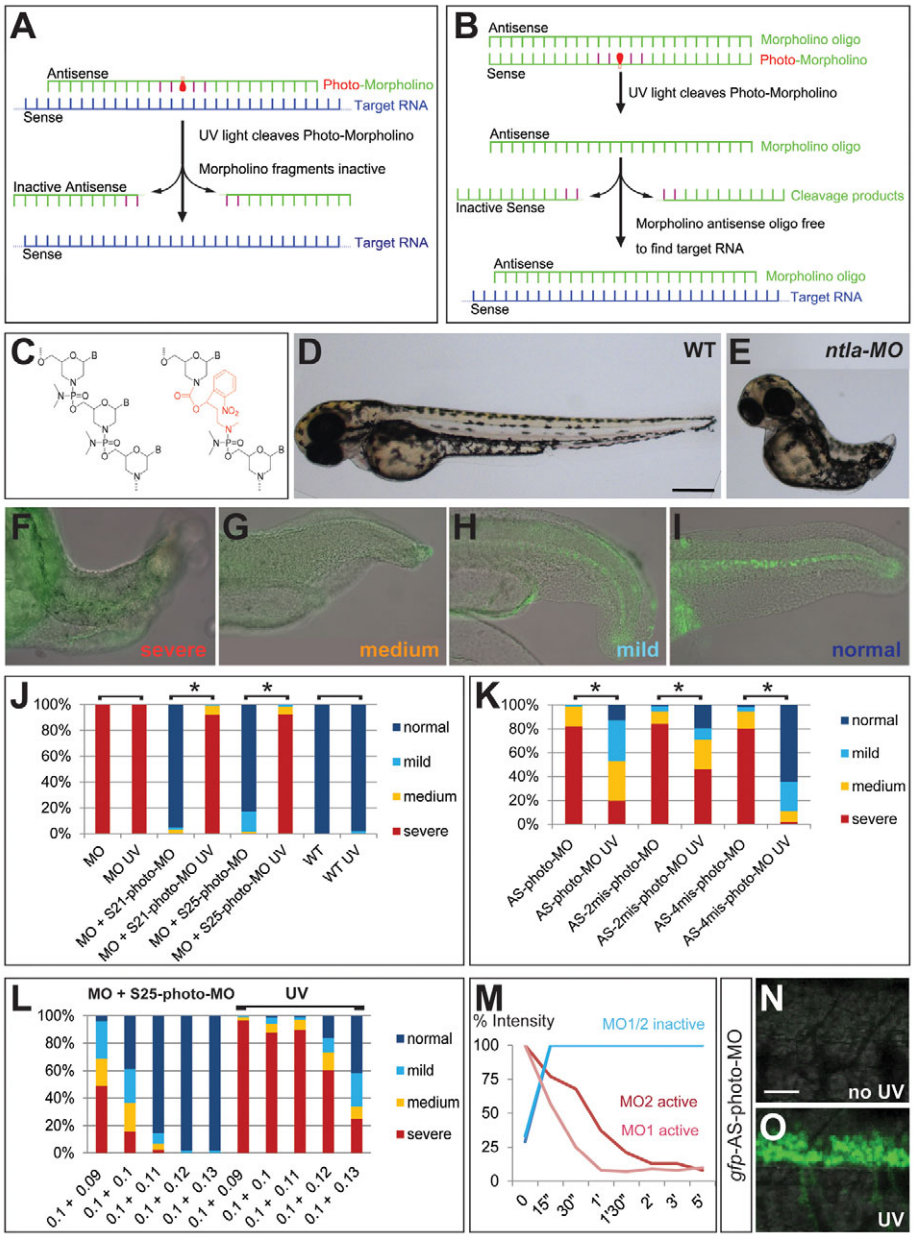

Fig. 1. S-photo-MO and AS-photo-MO regulate Ntla function. (**A**,**B**) Diagrams describing the mechanism of AS-photo-MO (A) and S-photo-MOs (B). (**C**) Molecular structure of the photo-subunit (red) and its position within the MO (green). (**D**,**E**) Lateral view of a wild-type embryo (D) and an *ntla*-MO injected embryo, missing posterior trunk and tail (E) at 48 hpf. Scale bar: 250 μm. (**F-I**) Overlays showing bright field and anti-Ntla labeling (green) in injected embryos at 26-28 hpf. Examples of severe (F), medium (G), mild (H) and normal (I) phenotypes. (**J-L**) Graphs showing percentage of embryos injected with MOs and photo-MOs resulting in severe (red), medium (orange), mild (light blue) and normal (dark blue) phenotypes, based on morphology. (J) *ntla*-S-photo-MOs of a length of 21 nucleotides (S21-photo-MO) and/or 25 nucleotides with four mismatches (S25-photo-MO) allow or block protein formation dependent on UV exposure. MO, n=60; MO UV, n=179; MO+S21-photo-MO, n=58; MO+S21-photo-MO UV, n=125; MO+S25-photo-MO, n=61; MO+S25-photo-MO UV, n=116; WT, n=114; WT UV, n=135. (K) All *ntla*-AS-photo-MO tested sufficiently block *ntla* gene function. Introducing two mismatches on either side of the photo-subunit (AS-4mis-photo-MO) significantly improved dissociation rate from the target and therefore recovery (P<0.05) of the phenotype after photo-cleavage compared with AS-photo-MO. AS-photo-MO, n=84; AS=photo=MO UV, n=132; AS-2mis-photo-MO, n=113; AS-2mis-photo-MO UV, n=134; AS-4mis-photo-MO, n=112; AS-4mis-photo-MO UV, n=152. Asterisks indicate significant differences (P<0.05) between untreated and UV-treated embryos. Student's t-test includes data in groups 'severe' and 'normal'. (L) Distribution of phenotypes after injecting different ratios of *ntla*-MO to S25-photo-MO solutions. The horizontal bar marks samples exposed to UV. (**M**) Quantification of in vitro mass spectroscopy analyses showing percentage of intensity of active (intact photo-element, red, pink) and inactive (cleaved photo-element, blue) *ntla*- or *gfp*-AS-photo-MOs, MO1 and MO2 respectively, measured over time after UV exposure. (**N**,**O**) Embryos injected with *gfp*-AS-photo-MO without UV exposure (N) and with UV exposure (O). Scale bar: 30 μm.

bases (supplementary material Table S1) for binding and dissociation properties. *ntla*-S-photo-MOs shorter than 21 nucleotides (supplementary material Table S1), even in fivefold excess, failed to sufficiently block *ntla*-MO and resulted in <3% normal embryos (n=268). Embryos injected with *ntla*-S-photo-MOs consisting of 21 nucleotides or 25 binding nucleotides with a

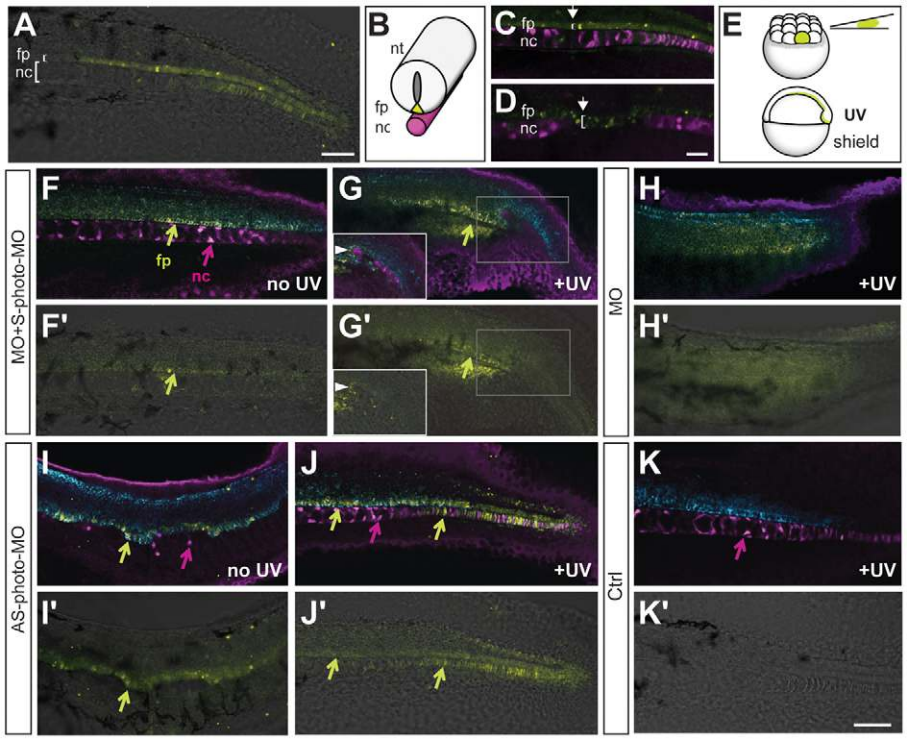

Fig. 2. Spatially restricted control of gene function using S- or AS-photo-MOs confirms *ntla*-dependent cell fate choice of MPCs. (**A**) Lateral view of live 28 hpf embryo highlighting notochord (nc) and floor plate (fp), created by a mosaic distribution of fluorescein-labeled control MO (yellow). (**B**) Cartoon showing neural tube (nt), fp (yellow) and underlying nc (magenta). (**C**,**D**) Distribution of fp cells (fluorescein, yellow) and Ntla antibody labeling in the notochord (magenta) in wild-type embryo (C) and *ntla*-MO-injected embryo lacking Ntla in some cells (arrow in D), leading to excess fp at the expense of notochord (compare extent of brackets). (**E**) Mosaic distribution of MO in non-neural tissues by injecting into one marginal cell of a 16-cell embryo. Embryos were exposed to UV at shield stage. (**F-J'**) Embryos show fluorescence (MO-fluorescein, yellow) in fp and/or notochord, Ntla (magenta) in notochord and zrf1 (cyan) staining in fp and neural tube. (G,G′) Inset in the bottom left corner shows a different *z* plane of the region marked by a gray box. Arrowheads point to the same Ntla-positive cell. (**K**,**K'**) Uninjected control embryo showing normal Ntla (magenta) and zrf1 (cyan) staining. (F-K′) Images show bright field and fluorescence labeling at 26-28 hpf. Embryos were injected with MO or photo-MOs as indicated and subjected to UV exposure as indicated (no UV, +UV). Scale bars: 30 μm for C,D; 50 μm for A,F-K′.

4 bp mismatch next to the photo-subunit resulted in ~95% normal phenotype when not exposed to light, and >90% severe phenotype with light exposure at 5 hpf (Fig. 1J).

We found that *ntla*-AS-photo-MOs blocked *ntla* gene function as well as *ntla*-MO did, but showed different binding and dissociation dynamics compared with *ntla*-S-photo-MOs and often continued to result in mutant phenotypes (Fig. 1J,K). This suggested that *ntla* expression was still being repressed to a limited extent after UV exposure. Release properties might be negatively affected by reaction of the photo-subunit cleavage product with the mRNA strand.

Introduction of mismatched bases on both sides of the photo-subunit significantly improved the dissociation dynamics of the *ntla*-AS-photo-MO (Fig. 1K). Despite its ability to completely block *ntla* function at 0.6 mM (AS-4mis-photo-MO) or 0.3 mM (AS-2mis-photo-MO), we lowered the concentration of the *ntla*-AS-photo-MOs to 0.4 mM (AS-4mis-photo-MO) and 0.2 mM (AS-2mis-photo-MO), respectively, to improve dissociation after UV exposure, leading to >60% wild-type phenotype. Without UV exposure, clutches of embryos showed 70-90% severe phenotypes (Fig. 1K). Embryos of the same clutch exposed to UV light showed 63-90% normal phenotype (Fig. 1K).

We emphasize that the correct ratio of *ntla*-MO/S-photo-MO was crucial for optimal binding and dissociation performance. A ratio of 1:1 *ntla*-MO to S-photo-MO consistently blocked *ntla* function and embryos developed normally after light exposure. Even minimal changes in the established ratio led to either an increase of *ntl* mutant phenotype without UV exposure or a reduction in *ntl* phenotype after UV exposure (Fig. 1L). Variability between experiments was <12% (Fig. 1J,K; coefficient of variation: 0.055-0.12) when we used pre-mixed *ntla*-MO/S-photo-MO stocks. MOs have been reported to result in cytotoxic effects (Eisen and Smith, 2008). Injection of MO or MO together with S-photo-MO and UV exposure did not significantly increase the proportion of embryos with cell death (<10% for all conditions, n=10 experiments, P>0.3 for all comparisons, Student's t-test).

In vitro analyses of UV photolysis by mass spectroscopy show that the photo-element of the AS-photo-MOs are completely cleaved within 2 minutes (n=3; Fig. 1M; supplementary material Fig. S2). In vivo analyses of injected embryos suggested sufficient cleavage after ~5 minute UV exposure. We followed onset of GFP expression in single live embryos over time and observed a faint fluorescent signal about 1 hour after UV exposure using *gfp*-AS-photo-MO or after 2 hours using *gal4*-AS-photo-MO, that became more prominent over time (Fig. 1N,O; supplementary material Fig. S2). The delay in onset of GFP expression after cleaving the photo-element of the *gal4*-AS-photo-MO is likely to be due to the time it takes for sequential translation of Gal4 and then the UAS-dependent GFP.

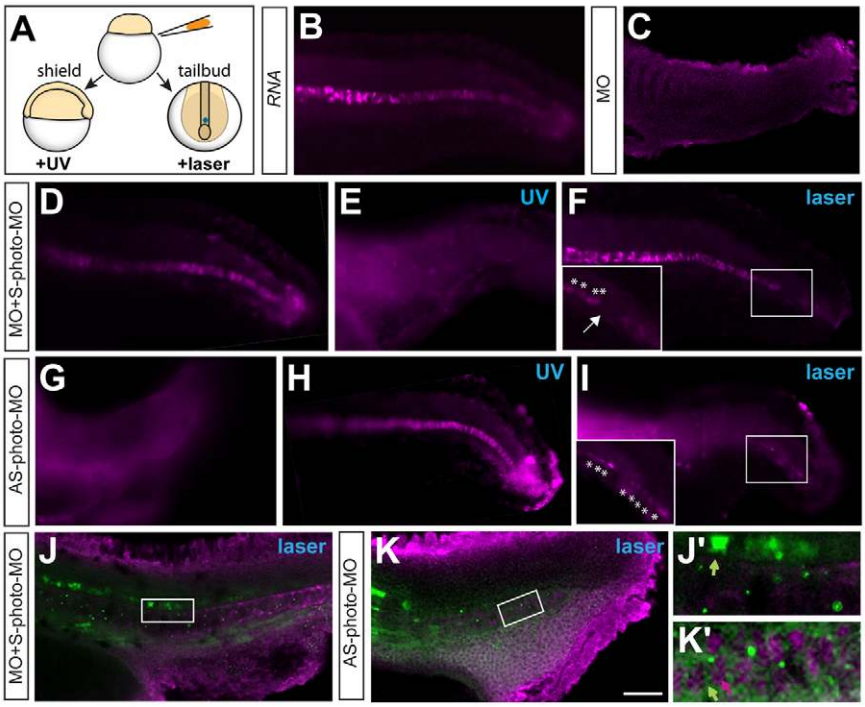

Fig. 3. Comparison of ubiquitous or cell-specific control of *ntla* gene function. (**A**) Embryos were injected with MOs at the one-cell stage. One group of embryos was exposed to light at 5 hpf, whereas in the other group, single cells within the MPCs were exposed to light at 11 hpf using a laser. (**B**) Normal Ntla protein distribution in embryos injected with *gfp* RNA as control. (**C-I**) Ntla labeling in transgenic embryos *Tg(hsp70:Gal4-VP16, UAS:GFP)* injected with MO or photo-MOs exposure as indicated. Embryos were treated with broad spectrum light (UV), kept in dark (no text) or exposed to laser (laser) as indicated. (F) Cells with photo-cleaved *ntla*-S-photo-MO lack Ntla labeling (arrow). Inset shows magnification of boxed area. Asterisks highlight Ntla expression in non-exposed cells. (I) Cells with photo-cleaved *ntla*-S-photo-MO show Ntla labeling, marked by asterisks. Inset shows magnification of boxed area. (**J-K′**) Embryos labeled for GFP (green) and Ntla (magenta) highlight cell fate of light exposed cells. J′ and K′ show higher magnifications of the boxed regions in J and K, respectively. (J′) Green arrow points to an fp cell (fluorescein, green). (K′) Green arrow indicates fluorescein labeling in cytosol and magenta arrow indicates Ntla labeling in the nucleus within cells in the nc. Scale bar: 50 μm.

Spatial and temporal control of *ntla* function

In wild-type zebrafish embryos, notochord and medial fp (Fig. 2A, yellow) both develop from MPCs (Appel et al., 1999; Halpern et al., 1993; Le Douarin and Halpern, 2000). fp cells form the ventral midline of the neural tube (Fig. 2B, yellow) and notochord forms a rod-like structure underlying the neural tube (Fig. 2B, magenta). Reduction of *ntla* expression in a limited number of MPCs by injecting *ntla*-MO into a single cell of a 16-cell stage embryo (Fig. 2E) resulted in these cells adopting an fp fate (yellow) at the expense of notochord (Fig. 2D, magenta). In wild type, medial fp consists of only one row of cells (Fig. 2C, bracket), whereas in the absence of Ntla we found multiple rows of cells forming fp (Fig. 2D, bracket) (see also Halpern et al., 1997).

To analyze further the spatial and temporal control of notochord formation by Ntla, we generated a mosaic distribution of photo-MOs selectively in non-neural tissues as described above and exposed embryos to UV at 5 hpf to cleave the photo-MO (Fig. 2E). Fluorescein-tagged MOs enabled identification of targeted cells. We performed immunofluorescence labeling on embryos selected by fluorescein fluorescence exclusively in notochord and/or fp at 26-28 hpf. We labeled fp (zrf-1) and Ntla (Fig. 2B) with antibodies, enabling us to compare their distributions in manipulated embryos. *ntla*-S-photo-MO sufficiently blocked *ntla*-MO (Fig. 2F,F′), allowing MPCs to develop normally, leading to fluorescent cells forming fp and notochord, and normal Ntla distribution in the notochord, similar to control embryos (Fig. 2K,K′). By contrast, in embryos exposed to UV light, we found fluorescein fluorescence exclusively in fp (Fig. 2G,G′). We confirmed deficiency of Ntla in these embryos (Fig. 2G,G′), similar to embryos injected with *ntla*-MO (Fig. 2H,H′). This suggests that all targeted MPCs might have adopted an fp fate at the expense of notochord owing to lack of Ntla protein.

Embryos injected with *ntla*-AS-photo-MO lacked all or most notochord (Fig. 2I,I′), with fluorescein-labeled cells exclusively forming fp. By contrast, embryos exposed to UV light developed normally, with fluorescein-labeled cells forming fp and Ntla-positive notochord (Fig. 2J,J′). The photo-MOs did not result in any effect on notochord development when progeny of the MO-injected cells gave rise to neural tissue (not shown). These results suggest that expression of *ntla* in MPCs at 5 hpf is sufficient for notochord induction (see also Ouyang et al., 2009).

Cell-specific temporal and spatial control of gene function

To examine further the cell-autonomous function of *ntla* and the photo-MOs, we used a UV laser at 11 hpf to illuminate a single cell. We injected *ntla*-photo-MOs into single-cell stage transgenic embryos carrying GFP under control of the heatshock promoter *Tg(hsp70:Gal4-VP16,UAS:GFP)*, and exposed a single cell or a group of three cells within the MPC domain to UV using a dye laser (365 nm; Fig. 3A). Laser exposure induced GFP expression and simultaneously cleaved the photo-MO. As a control, we exposed injected embryos to UV light at 5 hpf, similar to previous experiments. All embryos were analyzed further at 26-28 hpf using microscopy and antibody labeling for Ntla.

Embryos injected with RNA (encoding GFP) as a control showed normal Ntla protein expression (Fig. 3B), whereas embryos injected with *ntla*-MO lacked Ntla protein labeling (Fig. 3C). *ntla*-S-photo-MOs sufficiently blocked *ntla*-MO, allowing normal embryonic development when not exposed to UV (Fig. 3D). By contrast, UV light exposure at 5 hpf released *ntla*-MO resulting in severe *ntla* phenotypes (Fig. 3E). Spatially restricted activation of a MPC at 11 hpf resulted in absence of Ntla protein within the posterior tail region (Fig. 3F, arrow in inset).

We further determined that *ntla*-AS-photo-MOs sufficiently blocked Ntla protein formation (Fig. 3G) and allowed Ntla protein to be made after exposure to UV light at 5 hpf (Fig. 3H). Laser activation of MPCs at 11 hpf resulted in mosaic distribution of Ntla protein in the posterior trunk region (Fig. 3I, asterisks in inset). Furthermore, we noticed that these embryos formed more posterior

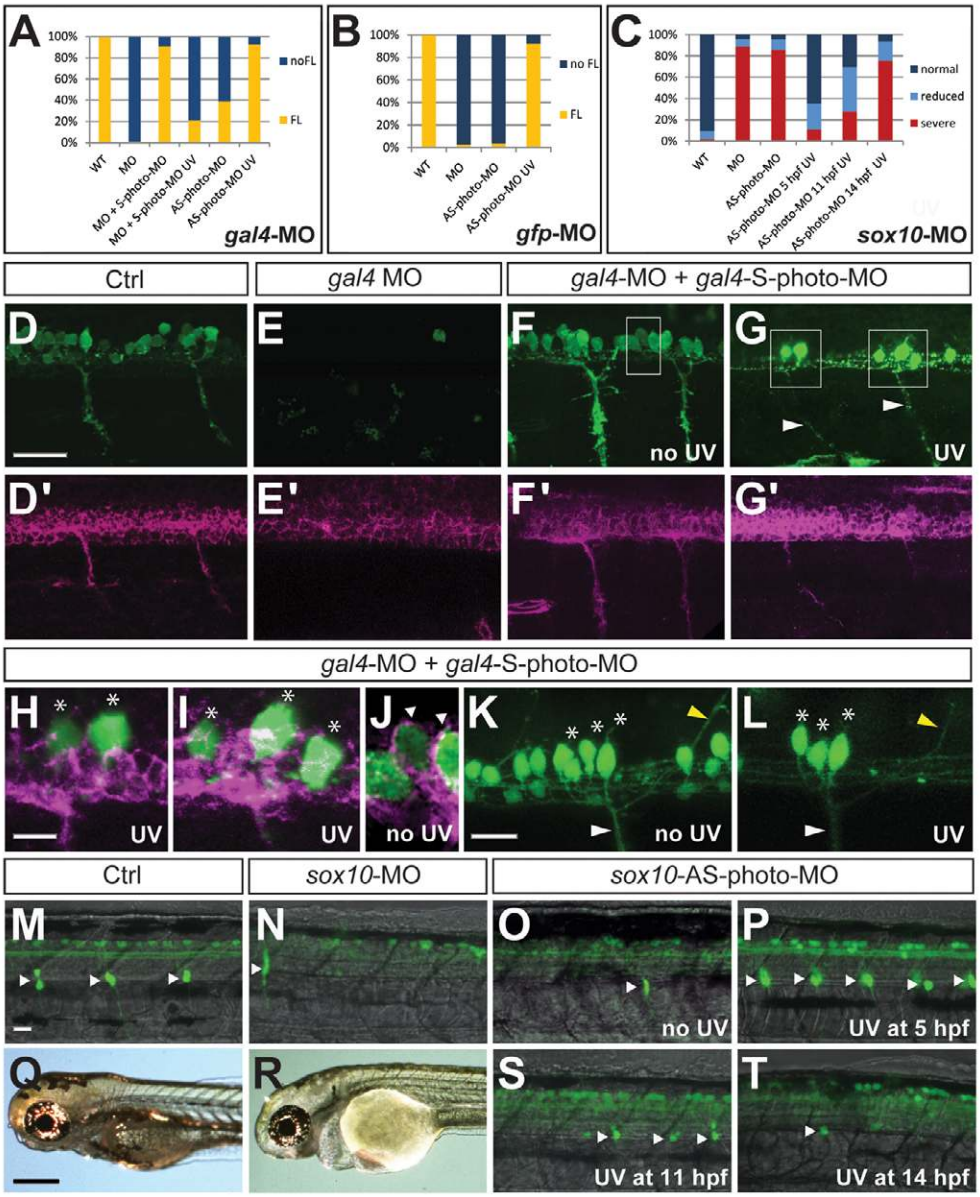

Fig. 4. Temporal control of photo-cleavable morpholinos. (**A**,**B**) Percentage of embryos expressing fluorescent protein (FL; fluorescent, orange) compared with 'non-glowers' (no FL; non-fluorescent, blue). (A) Embryos injected with MOs targeting *gal4* function and exposed to UV as indicated on the *x*-axis. WT, *n*=315; MO, *n*=179; MO+S-photo-MO, *n*=91; MO+S-photo-MO UV, *n*=99; AS-photo-MO, *n*=46; AS-photo-MO UV, *n*=90. (B) Embryos injected with MOs blocking GFP formation and exposed to UV as indicated on the *x*-axis. WT, *n*=144; MO, *n*=107; AS-photo-MO, *n*=106; AS-photo-MO UV, *n*=149. (**C**) Percentage of embryos with indicated pigment phenotype observed in *sox10*-MO injected embryos. MOs used and UV exposure are described on the *x*-axis. WT, *n*=81; MO, *n*=27; AS-photo-MO, *n*=58; AS-photo-MO 5hpf UV, *n*=44; AS-photo-MO 11hpf UV, *n*=48; AS-photo-MO 14hpf UV, *n*=35. Severe (red), no or only some pigment cells at 48 hpf; reduced (light blue), slightly diminished number of pigment cells compared with uninjected controls (normal, dark blue). (**D-G'**) Side view of two segments of *Tg(mnx1:gal4,UAS:GFP)* embryos at 26 hpf stained with anti-GFP (D-G, green), labeling all motoneurons or Alcama (D'-G', magenta), labeling only SMNs in uninjected control embryo (D,D'), embryo injected with *gal4*-MO (E,E') and embryo injected with *gal4*-MO/*gal4*-S-photo-MO (F,F'). (F) Embryos without UV exposure resemble normal GFP expression pattern. (G) GFP expression exclusively in PMNs in embryo exposed to UV at 14 hpf (G,G'). The image in G has been enhanced compared with F to improve visibility of PMN axons (see arrowheads). (**H-J**) High magnification of boxed regions in F (H) and G (I,J). (H,I) GFP-expressing neurons are not co-labeled with the SMN marker Alcama. (J) The margins of GFP-expressing neurons are labeled with Alcama. Arrowheads point to co-labeling of GFP (green) in the cytosol and Alcama (purple) in the membrane. (H-L) Asterisks indicate PMN cell bodies. (**K,L**) Live images of embryos without (K) and with (L) UV exposure. Location and axon trajectory identify GFP-expressing neurons as motoneurons. White arrowheads mark ventral projections, yellow arrowheads mark dorsal projections. Asterisks mark PMNs. (**M-T**) Embryos injected with *sox10*-MO (N-T) and uninjected control embryo (M). (M-P,S,T) Lateral views of three to four hemisegments in *Tg(3.1neurog1:GFP)* embryos expressing GFP in dorsal Rohon-Beard neurons and laterally located DRG neurons (arrowheads) at 3 dpf. Severely reduced number of DRG neurons in *sox10*-MO injected embryo (N) and *sox10*-AS-photo-MO injected embryo without UV exposure (O) compared with control embryo (M). UV exposure at 5 hpf leads to normal DRG development (P). UV exposure at 11 hpf leads to partial recovery of DRG formation (S), UV exposure at 14 hpf leads to severe reduction of DRG neurons (T). (Q,R) Severe reduction in pigment cells in *sox10*-MO injected embryo (R) compared with control embryo (Q), shown at 3 dpf. Scale bars: 30 μm for D-G',M-P,S,T; 7.5 μm for H-J; 15 μm for K,L; 300 μm for Q,R.

somites in the trunk compared with *ntla* mutant embryos (Fig. 3I), in agreement with previous reports using transplants (Martin and Kimelman, 2008).

Identification of the laser-exposed cells by examining GFP fluorescence in response to heatshock promoter activation revealed that Ntla expression was indeed exclusively localized to fp and not notochord, consistent with the lack of Ntla protein in these cells (Fig. 3J,J′). This is in agreement with previous transplant studies (Amacher et al., 2002; Halpern et al., 1993; Martin and Kimelman, 2008), suggesting that Ntla-deficient MPCs adopted a fp fate. In embryos injected with *ntla*-AS-photo-MO, laser-exposed cells populated notochord and fp (Fig. 3K,K′), suggesting that initial expression of *ntla* as late as 11 hpf in isolated MPCs induced these cells to form notochord and that MPCs are bipotent.

Temporal control over the Gal4-UAS system

Tools to genetically manipulate earlier-forming PMNs, but not later-forming SMNs, have been lacking, as there are no genes or promoters known to express exclusively in PMNs. PMNs begin to extend axons by 15 hpf (Flanagan-Steet et al., 2005). By contrast, SMNs do not extend axons until the end of segmentation (~24 hpf) (Lewis and Eisen, 2003). Thus, we considered using temporal regulation of Gal4 or GFP expression in a transgenic line of zebrafish [*Tg(mnx1:gal4, UAS:GFP)*] that expresses GFP in a Gal4-dependent way in both PMNs and SMNs.

First, we tested the ability of photo-cleavable MOs to control function of *gal4* and *gfp* using two transgenic lines expressing GFP under control of the Gal4-UAS system and assayed MO efficiency by the presence (FL, orange in Fig. 4A,B) or absence of fluorescent signal (no FL, blue; for examples of expression patterns see supplementary material Fig. S3). Without UV exposure >90% of embryos injected with *gal4*- or *gfp*-MO+S-photo-MO (Fig. 4A,B) showed fluorescence. Less than 20% of the embryos exposed to UV light exhibited fluorescence. Without UV, *gal4*-AS-photo-MOs blocked fluorescent expression in ~60% of embryos (Fig. 4A), whereas *gfp*-AS-photo-MOs were more efficient, blocking fluorescence in almost all embryos (Fig. 4B). About 95% of embryos showed fluorescent signal after exposure to UV light.

We chose to then block Gal4-mediated transcriptional activation of GFP expression by exposing *gal4*-MO/*gal4*-S-photo-MO-injected *Tg(mnx:gal4,UAS:GFP)* embryos to UV at 14 hpf. This manipulation allowed GFP expression in PMNs, but blocked expression in SMNs (Fig. 4G). We found that almost all SMNs lacked GFP expression (Fig. 4H,I), suggested by the absence of co-labeling with the SMN marker Alcama. We confirmed the presence of at least two types of PMNs by their ventral and dorsal projections (Fig. 4G,K,L, arrowheads). Embryos not exposed to UV developed normally (Fig. 4F), similar to control embryos (Fig. 4D), exhibiting GFP expression in Alcama-positive SMNs (Fig. 4J). As a control, *gal4*-MO injection resulted in almost no fluorescent signal in all motoneurons (Fig. 4E), and did not perturb the formation of SMNs (Fig. 4D′-G′). Thus, this application allows observation or manipulation specifically of PMNs during development.

Temporal control of *sox10* function

To examine the feasibility of using AS-photo-MOs to block and then release gene expression, we examined whether *sox10*, an important gene during neural crest development, is necessary for formation or maintenance of neural crest cells. First, to test the ability of photo-MOs to control *sox10* function, we assayed for the presence of pigment cells in *sox10*-AS-photo-MO-injected embryos and observed three different phenotypes, with ‘severe’ (red), slightly ‘reduced’ (light blue) or ‘normal’ (blue) number of pigment cells (Fig. 4C). We found that AS-photo-MOs, similar to *sox10*-MOs, prevented the formation of almost all pigment cells in ~90% of embryos. We blocked *sox10* function early during development using *sox10*-AS-photo-MO and allowed Sox10 protein to be made at later stages by cleaving the photo-element of the *sox10*-AS-photo-MO (Fig. 4C,M-T). Depending on the time of UV light exposure, we found a nearly normal number of pigment cells. Only 11% lacked pigment cells when exposed at 5 hpf, but 78% lacked pigment cells when exposed at 14 hpf.

In addition to analyzing the formation and migration of pigment cells, we also analyzed another population of neural crest derivatives, dorsal root ganglion (DRG) cells, in UV versus non-UV treated embryos at 2-3 dpf. The formation and migration of pigment cells and DRG cells was affected by AS-photo-MO and UV exposure similarly to pigment cells (Fig. 4O,P,S,T; data not shown). We describe the observed DRG phenotype in more detail in Fig. 4M-P,S,T.

Embryos injected with *sox10*-MO (Fig. 4N,R) or *sox10*-AS-photo-MO without UV treatment (Fig. 4O) exhibited a severe reduction in pigment and DRG neuron numbers compared with control embryos (Fig. 4M,Q). We exposed embryos to UV at 5, 11 and 14 hpf to narrow down the time in which *sox10* might be necessary for pigment and DRG development. When exposed early, at 5 hpf, both neural crest derivatives developed normally (Fig. 4P). UV exposure at 11 hpf led to partially restored pigment and DRG phenotype (Fig. 4C,S). Embryos exposed to UV at 14 hpf or later mostly lacked pigment cells and DRG neurons (Fig. 4T), similar to *sox10*-MO-injected embryos (Fig. 4N). Our results support the hypothesis that Sox10 is not required for early neural crest formation, but is important for later aspects of neural crest development. Further detailed analyses are necessary to fully understand the critical time period of Sox10 function in neural crest development.

DISCUSSION

MOs have proven to be useful tools for examining molecular mechanisms of development in a variety of animal models (Deiters et al., 2010). However, just as with mutations, if a gene has both early and late functions, blocking the early function with MOs often precludes studying the late function. Several studies have improved upon this system by developing MOs whose functions can be initially blocked and then released upon UV illumination (Deiters et al., 2010; Shestopalov and Chen, 2010; Shestopalov et al., 2007; Tomasini et al., 2009), providing one type of temporal control over MO activity. We have taken this one step further and here provide evidence for temporal control of MO function by activation and inactivation of MOs using light application in developing zebrafish embryos. Furthermore, we show the ability to regulate MOs in a limited number of cells, thus providing spatial control of MO function. With these new tools it will now be possible to examine when and where gene function is necessary or sufficient for normal developmental and physiological processes.

We show that the photo-element is completely cleaved by UV light within minutes (Fig. 1M) and that the onset of gene expression is consistent with immediate translation (~1 hour for GFP, supplementary material Fig. S2E). The best results are seen with photo-MOs that incorporate base pair mismatches on both sides of the photo-element (Fig. 1K). We show further that

function of the combined AS- and S-photo-MO is optimal at an equimolar ratio. We found that the MO/S-photo-MO ratio has to be precisely adjusted for every MO pair, and even small deviations from the optimal ratio can lead to significant changes in efficiency (Fig. 1L).

Our experiments demonstrate that the photo-subunit is not toxic to embryonic zebrafish. We observed that one of the *ntla* S-photo-MOs tested caused abnormal hindbrain development (not shown). However, removing the photo-element caused a similar phenotype, suggesting that the sense MO itself might perturb normal development unrelated to Ntla function in the mesoderm. Moving the *ntla* MO targeting sequence and the S-photo-MO to a region more upstream resulted in phenotypes specific to *ntla* function. These experiments demonstrate that some photo-MOs, similar to some conventional MOs (Eisen and Smith, 2008), can cause off-target effects and, importantly, that the photo-element did not contribute to toxicity.

The Gal4-UAS transgenesis system for directing transgene expression has recently become commonly used in zebrafish (Halpern et al., 2008; Scott, 2009). We show that photo-cleavable *gal4*-MOs enable temporal control over *gal4*-dependent effector genes, here GFP, providing the potential for temporal control and cell-type specificity in many existing Gal4-UAS transgenic lines (Scott et al., 2007). Some Gal4-VP16 driver lines, as demonstrated for *Tg(UAS:myc-Notch1a-intra)kca3* crossed to the *Et(–1.5hsp70l:Gal4-VP16)s1006t* line, show non-specific background expression in tissues unrelated to endogenous gene expression (Faucherre and Lopez-Schier, 2011) and unspecific morphological defects, which might be caused by leakiness of the heat-shock promoter used in the effector line. Blocking Gal4 function early using a *gal4*-MO prevented background GFP expression as well as all morphological abnormalities (Faucherre and Lopez-Schier, 2011). Using regular MOs allowed some dose-dependent temporal control over Gal4 function, probably based on dilution of the MO to ineffective doses at later stages of development (2-6 dpf) (Eisen and Smith, 2008; Faucherre and Lopez-Schier, 2011). Photo-cleavable MOs should dramatically improve control over Gal4-mediated gene expression.

Another application for delaying MO activity might lie in studying genes with functions at multiple times during development. It was shown that maternally contributed E-cadherin mRNA is crucial during early mouse development (Kanzler et al., 2003), preventing developmental arrest. Similar to mouse, zebrafish E-cadherin (*cdh1*) is maternally contributed and was shown to be required for gastrulation cell movements, with the absence of *cdh1* causing epiboly arrest (Shimizu et al., 2005). The expression of *cdh1* in specific regions within the developing brain at later stages (Babb et al., 2001) suggests an additional later function during neural development, corroborated by studies in mouse cell culture (Fiederling et al., 2011; Shimamura and Takeichi, 1992). Blocking late, and not early, expression using photo-cleavable MOs could now allow direct investigation of the role of *cdh1* in neural development.

In summary, we demonstrate that light-sensitive photo-MOs are valuable tools for studying gene function in a temporally and spatially restricted manner. S-photo-MOs block commonly used MOs allowing temporal inactivation of gene function. Light exposure releases the MO, resulting in knockdown of gene function. We report for the first time the use of a light sensitive AS-photo-MO that temporarily blocks protein formation. Normal gene function can be restored by light-induced inactivation of the AS-photo-MO.

Acknowledgements
We thank Fiona Wardle for sharing the Ntla antibody; Herwig Baier for providing *Et[(–1.5hsp70l:Gal4-VP16)s1102t,(UAS-E1b:Kaede)s1999t]* fish; and Jamie Nichols for helpful comments on the manuscript.

Funding
This work was supported by grants from the National Institutes of Health (NIH) [R01NS065795 to P.W., R01NS23915 to J.E. and P01HD22486 to P.W. and J.E.]. Deposited in PMC for immediate release.

Competing interests statement
A.T., D.G., S.S., J.E. and P.W. declare no competing financial interests. P.M. and Y.L. are employees of Gene Tools, LLC. They designed and synthesized the MOs and photo-MOs used in this study and provided mass spectroscopy analysis. They were not involved in experimental design, analysis or writing of the manuscript.

Supplementary material
Supplementary material available online at
http://dev.biologists.org/lookup/suppl/doi:10.1242/dev.072702/-/DC1

References
Amacher, S. L., Draper, B. W., Summers, B. R. and Kimmel, C. B. (2002). The zebrafish T-box genes no tail and spadetail are required for development of trunk and tail mesoderm and medial floor plate. *Development* **129**, 3311-3323.
Appel, B., Fritz, A., Westerfield, M., Grunwald, D. J., Eisen, J. S. and Riley, B. B. (1999). Delta-mediated specification of midline cell fates in zebrafish embryos. *Curr. Biol.* **9**, 247-256.
Babb, S. G., Barnett, J., Doedens, A. L., Cobb, N., Liu, Q., Sorkin, B. C., Yelick, P. C., Raymond, P. A. and Marrs, J. A. (2001). Zebrafish E-cadherin: expression during early embryogenesis and regulation during brain development. *Dev. Dyn.* **221**, 231-237.
Bill, B. R., Petzold, A. M., Clark, K. J., Schimmenti, L. A. and Ekker, S. C. (2009). A primer for morpholino use in zebrafish. *Zebrafish* **6**, 69-77.
Carney, T. J., Dutton, K. A., Greenhill, E., Delfino-Machin, M., Dufourcq, P., Blader, P. and Kelsh, R. N. (2006). A direct role for Sox10 in specification of neural crest-derived sensory neurons. *Development* **133**, 4619-4630.
Clark, K. J., Balciunas, D., Pogoda, H. M., Ding, Y., Westcot, S. E., Bedell, V. M., Greenwood, T. M., Urban, M. D., Skuster, K. J., Petzold, A. M. et al. (2011). In vivo protein trapping produces a functional expression codex of the vertebrate proteome. *Nat. Methods* **8**, 506-512.
Collins, R. T., Linker, C. and Lewis, J. (2010). MAZe: a tool for mosaic analysis of gene function in zebrafish. *Nat. Methods* **7**, 219-223.
Deiters, A., Garner, R. A., Lusic, H., Govan, J. M., Dush, M., Nascone-Yoder, N. M. and Yoder, J. A. (2010). Photocaged morpholino oligomers for the light-regulation of gene function in zebrafish and *Xenopus* embryos. *J. Am. Chem. Soc.* **132**, 15644-15650.
Dong, Q., Svoboda, K., Tiersch, T. R. and Todd Monroe, W. (2007). Photobiological effects of UVA and UVB light in zebrafish embryos: Evidence for a competent photorepair system. *J. Photochem. Photobiol. B* **88**, 137-146.
Eisen, J. S. and Smith, J. C. (2008). Controlling morpholino experiments: don't stop making antisense. *Development* **135**, 1735-1743.
Esengil, H., Chang, V., Mich, J. K. and Chen, J. K. (2007). Small-molecule regulation of zebrafish gene expression. *Nat. Chem. Biol.* **3**, 154-155.
Faucherre, A. and Lopez-Schier, H. (2011). Delaying Gal4-driven gene expression in the zebrafish with morpholinos and Gal80. *PLoS ONE* **6**, e16587.
Fiederling, A., Ewert, R., Andreyeva, A., Jungling, K. and Gottmann, K. (2011). E-cadherin is required at GABAergic synapses in cultured cortical neurons. *Neurosci. Lett.* **501**, 167-172.
Flanagan-Steet, H., Fox, M. A., Meyer, D. and Sanes, J. R. (2005). Neuromuscular synapses can form in vivo by incorporation of initially aneural postsynaptic specializations. *Development* **132**, 4471-4481.
Halpern, M. E., Ho, R. K., Walker, C. and Kimmel, C. B. (1993). Induction of muscle pioneers and floor plate is distinguished by the zebrafish no tail mutation. *Cell* **75**, 99-111.
Halpern, M. E., Hatta, K., Amacher, S. L., Talbot, W. S., Yan, Y. L., Thisse, B., Thisse, C., Postlethwait, J. H. and Kimmel, C. B. (1997). Genetic interactions in zebrafish midline development. *Dev. Biol.* **187**, 154-170.
Halpern, M. E., Rhee, J., Goll, M. G., Akitake, C. M., Parsons, M. and Leach, S. D. (2008). Gal4/UAS transgenic tools and their application to zebrafish. *Zebrafish* **5**, 97-110.
Kanzler, B., Haas-Assenbaum, A., Haas, I., Morawiec, L., Huber, E. and Boehm, T. (2003). Morpholino oligonucleotide-triggered knockdown reveals a role for maternal E-cadherin during early mouse development. *Mech. Dev.* **120**, 1423-1432.
Kelsh, R. N. (2006). Sorting out Sox10 functions in neural crest development. *BioEssays* **28**, 788-798.

Kimmel, C. B., Ballard, W. W., Kimmel, S. R., Ullmann, B. and Schilling, T. F. (1995). Stages of embryonic development of the zebrafish. *Dev. Dyn.* **203**, 253-310.
Le Douarin, N. M. and Halpern, M. E. (2000). Discussion point. Origin and specification of the neural tube floor plate: insights from the chick and zebrafish. *Curr. Opin. Neurobiol.* **10**, 23-30.
Lewis, K. E. and Eisen, J. S. (2003). From cells to circuits: development of the zebrafish spinal cord. *Prog. Neurobiol.* **69**, 419-449.
Marcus, R. C. and Easter, S. S., Jr (1995). Expression of glial fibrillary acidic protein and its relation to tract formation in embryonic zebrafish (*Danio rerio*). *J. Comp. Neurol.* **359**, 365-381.
Martin, B. L. and Kimelman, D. (2008). Regulation of canonical Wnt signaling by Brachyury is essential for posterior mesoderm formation. *Dev. Cell* **15**, 121-133.
Ouyang, X., Shestopalov, I. A., Sinha, S., Zheng, G., Pitt, C. L. W., Li, W.-H., Olson, A. J. and Chen, J. K. (2009). Versatile synthesis and rational design of caged morpholinos. *J. Am. Chem. Soc.* **131**, 13255-13269.
Schulte-Merker, S., Ho, R. K., Herrmann, B. G. and Nusslein-Volhard, C. (1992). The protein product of the zebrafish homologue of the mouse T gene is expressed in nuclei of the germ ring and the notochord of the early embryo. *Development* **116**, 1021-1032.
Schulte-Merker, S., van Eeden, F. J., Halpern, M. E., Kimmel, C. B. and Nusslein-Volhard, C. (1994). no tail (ntl) is the zebrafish homologue of the mouse T (Brachyury) gene. *Development* **120**, 1009-1015.
Scott, E. K. (2009). The Gal4/UAS toolbox in zebrafish: new approaches for defining behavioral circuits. *J. Neurochem.* **110**, 441-456.
Scott, E. K., Mason, L., Arrenberg, A. B., Ziv, L., Gosse, N. J., Xiao, T., Chi, N. C., Asakawa, K., Kawakami, K. and Baier, H. (2007). Targeting neural circuitry in zebrafish using GAL4 enhancer trapping. *Nat. Methods* **4**, 323-326.
Shestopalov, I. A. and Chen, J. K. (2010). Oligonucleotide-based tools for studying zebrafish development. *Zebrafish* **7**, 31-40.
Shestopalov, I. A., Sinha, S. and Chen, J. K. (2007). Light-controlled gene silencing in zebrafish embryos. *Nat. Chem. Biol.* **3**, 650-651.
Shimamura, K. and Takeichi, M. (1992). Local and transient expression of E-cadherin involved in mouse embryonic brain morphogenesis. *Development* **116**, 1011-1019.
Shimizu, T., Yabe, T., Muraoka, O., Yonemura, S., Aramaki, S., Hatta, K., Bae, Y. K., Nojima, H. and Hibi, M. (2005). E-cadherin is required for gastrulation cell movements in zebrafish. *Mech. Dev.* **122**, 747-763.
Strahle, U. and Jesuthasan, S. (1993). Ultraviolet irradiation impairs epiboly in zebrafish embryos: evidence for a microtubule-dependent mechanism of epiboly. *Development* **119**, 909-919.
Tomasini, A. J., Schuler, A. D., Zebala, J. A. and Mayer, A. N. (2009). PhotoMorphs: A novel light-activated reagent for controlling gene expression in zebrafish. *Genesis* **47**, 736-743.
Trevarrow, B., Marks, D. L. and Kimmel, C. B. (1990). Organization of hindbrain segments in the zebrafish embryo. *Neuron* **4**, 669-679.
Westerfield, M. (2000). *The Zebrafish Book.* Eugene OR: Institute for Neuroscience, University of Oregon.